Noble metal Free MoS$_2$/ZnIn$_2$S$_4$ nanocomposite for acceptorless photocatalytic semi-dehydrogenation of 1,2,3,4-tetrahydroisoquinoline to produce 3,4-dihydroisoquinoline

Mingming Hao, Xiaoyu Deng, Lizhi Xu, Zhaohui Li*

Research Institute of Photocatalysis, State Key Laboratory of Photocatalysis on Energy and Environment, College of Chemistry, Fuzhou University, Fuzhou, 350116, PR China

A B S T R A C T

MoS$_2$/ZnIn$_2$S$_4$ nanocomposite was prepared via photoreduction of (NH$_4$)$_2$MoS$_4$ in the presence of hexagonal ZnIn$_2$S$_4$. The as-obtained MoS$_2$/ZnIn$_2$S$_4$ nanocomposite showed superior activity for acceptorless photocatalytic semi-dehydrogenation of 1,2,3,4-tetrahydroisoquinoline to produce 3,4-dihydroisoquinoline, with quantitative hydrogen evolved. In addition to MoS$_2$/ZnIn$_2$S$_4$, a series of MS/ZnIn$_2$S$_4$ nanocomposites (MS = PtS and NiS) were also found to be active for this reaction, indicating that ZnIn$_2$S$_4$-based nanocomposites are effective photocatalysts for acceptorless semi-dehydrogenation of 1,2,3,4-tetrahydroisoquinoline to produce 3,4-dihydroisoquinoline. This study not only provides an efficient, green and cost effective strategy to produce 3,4-dihydroisoquinoline, but also highlights the great potential of semiconductor-based photocatalysis for light-driven organic syntheses.

1. Introduction

3,4-Dihydroisoquinoline plays an important role in the syntheses of pharmaceuticals [1,2]. For example, it is an important intermediate for the synthesis of morphinans and also a precursor to isoquinoline alkaloids, which are involved in many biological activities [3]. A straightforward method to obtain 3,4-dihydroisoquinoline is from 1,2,3,4-tetrahydroisoquinoline since it is a widely distributed alkaloid in nature [4]. The transformation of 1,2,3,4-tetrahydroisoquinoline to 3,4-dihydroisoquinoline can be realized either with the participation of an oxidant or in absence of the proton acceptors [5,6]. Acceptorless semi-dehydrogenation of 1,2,3,4-tetrahydroisoquinoline to produce 3,4-dihydroisoquinoline is especially useful not only because it can avoid the use of stoichiometric oxidants as the proton couplers in the reaction, but also can produce hydrogen concomitantly [7]. However, the semi-dehydronation of 1,2,3,4-tetrahydroisoquinoline is extremely challenging since the first and second oxidative potential of 1,2,3,4-tetrahydroisoquinoline (+1.01 V and +1.15 V vs. NHE), which corresponding to the dehydrogenation of two protons and four protons in 1,2,3,4-tetrahydroisoquinoline, respectively, is quite close. In addition, the formation of aromatized N-heterocycle also facilitates the complete dehydrogenation of four protons to form isoquinoline [8]. Most already reported strategies for the transformation of 1,2,3,4-tetrahydroisoquinoline to 3,4-dihydroisoquinoline therefore involves noble metal based nanocomposites or complexes [8–10] since the reverse process, ie, the hydrogenation of the isoquinoline to form 3,4-dihydroisoquinoline may coexist in these reaction systems. For these reaction systems, designed ligands and high temperature are sometimes also required [5]. Considering the scarcity of the noble metals and their high price, the associated tedious process in the synthesis of organic ligands and the recyclability of the catalysts, the development of a noble metal free highly efficient heterogeneous catalytic system for acceptorless semi-dehydrogenation of 1,2,3,4-tetrahydroisoquinoline to produce 3,4-dihydroisoquinoline would be highly desirable.

With an aim of developing sustainable processes for organic syntheses, recently heterogeneous photocatalytic organics transformations have received increasing attention [11–17]. Acceptorless photocatalytic dehydrogenation has developed rapidly not only because it can provide green and sustainable strategy for the synthesis of value-added organic compounds, but also due to its great potentials in hydrogen storage and transportation [8,18–22]. Acceptorless photocatalytic dehydrogenation of 1,2,3,4-tetrahydroisoquinoline to produce isoquinoline was recently reported by Wang's group over ternary h-BCN, a photocatalyst with a band gap of 2.7 eV and a positive enough valence band level to thermodynamically dehydrogenate of all four protons in 1,2,3,4-tetrahydroisoquinoline [23]. Considering the slightly

differentiated oxidative potentials of 1,2,3,4-tetrahydroisoquinoline, this study implies that the semi-dehydrogenation of 1,2,3,4-tetrahydroisoquinoline to generate 3,4-dihydroisoquinoline may be realized over a photocatalyst with a slightly milder oxidative capability as compared with *h*-BCN.

Ternary hexagonal $ZnIn_2S_4$, with a band gap of ca. 2.4 eV, has been well demonstrated to be a good photocatalyst for hydrogen evolution and organic transformations under visible light [24–27]. Considering that the valence band potential of hexagonal $ZnIn_2S_4$ locates at ca. 1.2 V vs NHE, the dehydrogenation of the first two protons in 1,2,3,4-tetrahydroisoquinoline to generate 3,4-dihydroisoquinoline with one molecule of H_2 evolved should go easily over irradiated $ZnIn_2S_4$, if coupled with suitable hydrogen evolution cocatalysts, since the first oxidative potential of 1,2,3,4-tetrahydroisoquinoline occurs at + 1.01 V vs NHE. However, the dehydrogenation of all four protons in 1,2,3,4-tetrahydroisoquinoline to produce isoquinoline should not be so favorable over irradiated $ZnIn_2S_4$ since it's valence band potential is quite close to the second oxidative potential of 1,2,3,4-tetrahydroisoquinoline (1.15 V vs NHE). Therefore, it is possible for the acceptorless photocatalytic dehydrogenation of 1,2,3,4-tetrahydroisoquinoline over irradiated $ZnIn_2S_4$ to stop in the semi-dehydrogenation stage to produce 3,4-dihydroisoquinoline.

MoS_2 has been reported to be an excellent cocatalyst for photocatalytic hydrogen evolution over a series of semiconductor-based photocatalysts [28–34]. In this manuscript, we reported the preparation of $MoS_2/ZnIn_2S_4$ nanocomposite via photoreduction of $(NH_4)_2MoS_4$ in the presence of preformed $ZnIn_2S_4$ microspheres under visible light. The as-obtained $MoS_2/ZnIn_2S_4$ nanocomposite showed superior photocatalytic activity for acceptorless semi-dehydrogenation of 1,2,3,4-tetrahydroisoquinoline to produce 3,4-dihydroisoquinoline. In addition to $MoS_2/ZnIn_2S_4$, several other $MS/ZnIn_2S_4$ nanocomposites (MS = NiS and PtS) obtained by deposition of chalcogenides-based cocatalysts on $ZnIn_2S_4$ also show superior activity for this reaction. This study not only provides an efficient, green and cost effective strategy for the production of 3,4-dihydroisoquinoline, but also highlights the great potential of semiconductor-based photocatalysis in organics syntheses.

2. Experimental

All the reagents are analytical grade and used without further purifications. Hexagonal $ZnIn_2S_4$ was prepared following a previously reported method [24]. Ammonium tetrathiomolybdate $((NH_4)_2MoS_4)$ was prepared from ammonium paramolybdate $((NH_4)_6Mo_7O_{24}\cdot4H_2O)$ and ammonium sulfide $((NH_4)_2S)$ following a previously reported method [35].

1.0 wt% $MoS_2/ZnIn_2S_4$ nanocomposite was obtained by photoreduction of $(NH_4)_2MoS_4$ in the presence of hexagonal $ZnIn_2S_4$. $ZnIn_2S_4$ (200 mg, 0.3 mmol) and $(NH_4)_2MoS_4$ (3 mg, 0.012 mmol) in a dry schlenk tube was degassed and filled with N_2. Degassed CH_3OH (3 ml) was injected into the schlenk tube. The schlenk tube was irradiated for 3 h with a 300 W Xe arc lamp (Beijing Perfect light, PLS-SXE300c). The resultant product was obtained by centrifuge, washed with deionized water and CH_3OH for several times, and dried overnight at 60 °C in an oven.

1.0 wt% $PtS/ZnIn_2S_4$ and 1.0 wt% $NiS/ZnIn_2S_4$ nanocomposites were obtained following previously reported methods [36,37].

3. Characterizations

The as-obtained products were characterized by X-ray diffraction (XRD) patterns on a D8 Advance X-ray diffractometer (Bruker) using Cu K_α (λ = 1.5406 Å) radiation at a voltage of 40 kV and 40 mA. XRD patterns were scanned over the angular range of 5 − 90° (2θ) with a step size of 0.02°. X-ray photoelectron spectroscopy (XPS) measurements were performed on a PHI Quantum 2000 XPS system (PHI, USA) with a monochromatic Al K_α source and a charge neutralizer. All the

binding energies were referenced to the C1s peak at 284.6 eV of the surface adventitious carbon. The transmission electron microscopy (TEM) and high resolution TEM (HRTEM) images were measured by JEOL model JEM 2010 EX instrument at an accelerating voltage of 200 kV. The UV–vis diffuse reflectance spectrum (UV–vis DRS) was obtained with a UV–vis spectrophotometer (Varian Cary 500). Barium sulfate $(BaSO_4)$ was used as a reference.

4. Catalytic reactions

The light induced semi-dehydrogenation reactions were carried out in a sealed schlenk tube irradiated with a photocatalytic parallel reaction device (PCX50B Discover, 5 W). For the semi-dehydrogenation of 1,2,3,4-tetrahydroisoquinoline, the catalyst (10 mg) and 1,2,3,4-tetrahydroisoquinoline (13 μL, 0.1 mmol) were suspended in reaction medium (2 ml). Before the reaction, the suspension was degassed and saturated with N_2 to remove any dissolved O_2. Then the reaction was performed under visible light with a photocatalytic parallel reaction device. After the reaction, the resultant suspension was filtered through a porous membrane (20 μm in diameter) and the filtrate was analyzed by GC–MS and GC-FID (Shimadzu GC-2014) equipped with an HP-5 capillary column. The gaseous products were analyzed by GC-TCD (Shimadzu GC-2014) with a TDX-01 packed column.

5. Results and discussion

Hexagonal $ZnIn_2S_4$ was obtained solvothermally from $ZnCl_2$ and $InCl_3$ in a mixed solvent of DMF and ethylene glycol (EG) following a previously reported method (Fig. 1a) [24]. $MoS_2/ZnIn_2S_4$ nanocomposite was obtained via photoreduction of $(NH_4)_2MoS_4$ over hexagonal $ZnIn_2S_4$ under visible light. Since the conduction band of hexaganol $ZnIn_2S_4$ locates at ca. -1.10 V vs NHE [38], more negative than the redox potential of MoS_4^{2+}/MoS_2 (-0.24 V vs NHE) [28], the reduction of $(NH_4)_2MoS_4$ to MoS_2 by photo-generated electrons of hexagonal $ZnIn_2S_4$ is thermodynamically favorable. Therefore upon irradiation, the photogenerated electrons in $ZnIn_2S_4$ reduce $(NH_4)_2MoS_4$ to form deposited MoS_2 on the surface of $ZnIn_2S_4$, while CH_3OH act as sacrificial electron donors to consume the left photogenerated holes in $ZnIn_2S_4$ to complete the whole photocatalytic cycle. A similar strategy by using CQDs as the photocatalyst for photoreduction of $(NH_4)_2MoS_4$ to *in-situ* synthesis of MoS_2 was previously reported [28]. The XRD patterns of the as-obtained $MoS_2/ZnIn_2S_4$ nanocomposite shows characteristic 2θ peaks of hexagonal $ZnIn_2S_4$, indicating that the photoreduction process does not destroy the phase of hexagonal $ZnIn_2S_4$ (Fig. 1b). No characteristic diffraction peaks corresponding to MoS_2 are observed, probably due to its low loading amount and its homogeneous dispersion in the nanocomposite. However, the presence of MoS_2 was
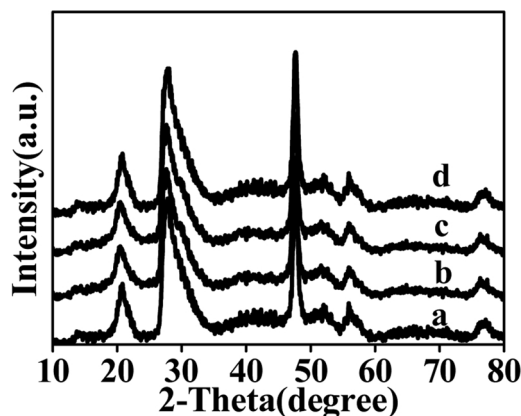
Fig. 1. XRD patterns of (a) bare $ZnIn_2S_4$; (b) 1.0 wt% $MoS_2/ZnIn_2S_4$; (c) 1.0 wt% $NiS/ZnIn_2S_4$; (d) 1.0 wt% $PtS/ZnIn_2S_4$ nanocomposites.
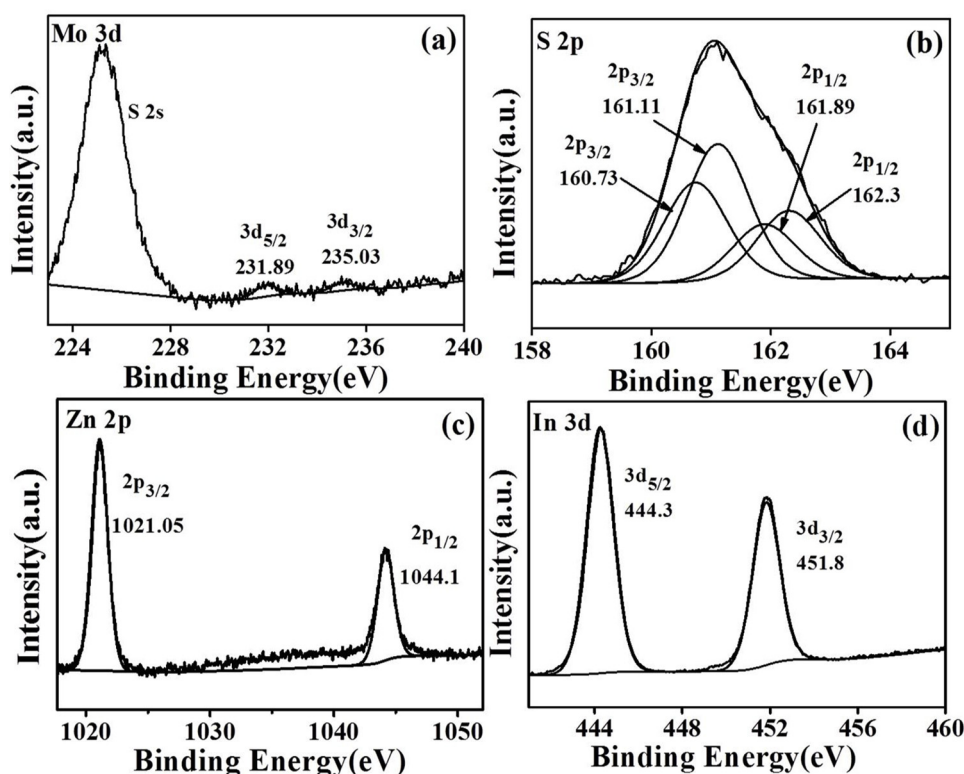
Fig. 2. XPS spectra of 1.0 wt% $MoS_2/ZnIn_2S_4$ nanocomposite in (a) Mo 3d region; (b) S 2p region; (c) Zn 2p region; (d) In 3d region.

confirmed by the XPS result of 1.0 wt% $MoS_2/ZnIn_2S_4$ nanocomposite by showing two peaks at 231.89 eV and 235.03 eV, attributable to Mo $3d_{5/2}$ and Mo $3d_{3/2}$, respectively (Fig. 2a). Accordingly, the XPS spectra in S 2p region can be deconvoluted into two sets of peaks, indicating that S exists in two different chemical environment (Fig. 2b). By comparison with bare $ZnIn_2S_4$, the peaks at 161.11 eV and 162.3 eV can be assigned to S $2p_{3/2}$ and S $2p_{1/2}$ in $ZnIn_2S_4$, while the other two peaks at 160.73 eV and 161.89 eV can be attributed to S $2p_{3/2}$ and S $2p_{1/2}$ in MoS_2, respectively. The XPS spectra of 1.0 wt% $MoS_2/ZnIn_2S_4$ nanocomposite also shows peaks at 1021.05 and 1044.1 eV for Zn $2p_{3/2}$ and Zn $2p_{1/2}$, as well as peaks at 451.8 and 444.3 eV corresponding to In $3d_{3/2}$ and In $3d_{5/2}$ (Fig. 2c and 2d). A high binding energy shift for both Zn 2p and In 3d peak, as compared with bare $ZnIn_2S_4$, is observed over $MoS_2/ZnIn_2S_4$ nanocomposite, indicating the existence of strong electronic interaction between MoS_2 and $ZnIn_2S_4$.

The TEM image of 1.0 wt% $MoS_2/ZnIn_2S_4$ nanocomposite shows that it consists of flower-like microspheres with a dimension of 1–3 μm, which are assembled by densely packed nanosheets (Fig. 3a). The HRTEM image shows clear lattice fringes of 0.32 nm matching that of (102) plane of hexagonal $ZnIn_2S_4$, as well as lattice fringes of 0.62 nm

corresponding to (002) plane of hexagonal MoS_2 (Fig. 3b).

The UV–vis spectrum of $MoS_2/ZnIn_2S_4$ nanocomposite shows strong absorption in the visible light, with the absorption edge extends to 500 nm, in consistent with the band gap of hexagonal $ZnIn_2S_4$. The deposition of MoS_2 on the surface of $ZnIn_2S_4$ leads to a slightly enhanced light absorption in the visible light region, ascribed to the absorption induced by the deposited MoS_2 (Fig. 4).

The performance of the as-obtained $MoS_2/ZnIn_2S_4$ nanocomposite for photocatalytic dehydrogenation of 1,2,3,4-tetrahydroisoquinoline was investigated under visible light. The reaction was initially carried out in H_2O. After irradiated for 12 h, 83% of 1,2,3,4-tetrahydroisoquinoline was transformed, with a yield of 81% to 3,4-dihydroisoquinoline and only 2% to isoquinoline. Almost quantitative amount of H_2 was also generated (Table 1, entry 1). No product was detected when the reaction was carried out in absence of either light or $MoS_2/ZnIn_2S_4$ nanocomposite (Table 1, entry 2–3), indicating that the dehydrogenation of 1,2,3,4-tetrahydroisoquinoline was induced by irradiated $MoS_2/ZnIn_2S_4$. When bare $ZnIn_2S_4$ was used, only 65% of 1,2,3,4-tetrahydroisoquinoline was converted, with a yield of 60% to 3,4-dihydroisoquinoline under similar conditions. This indicates that
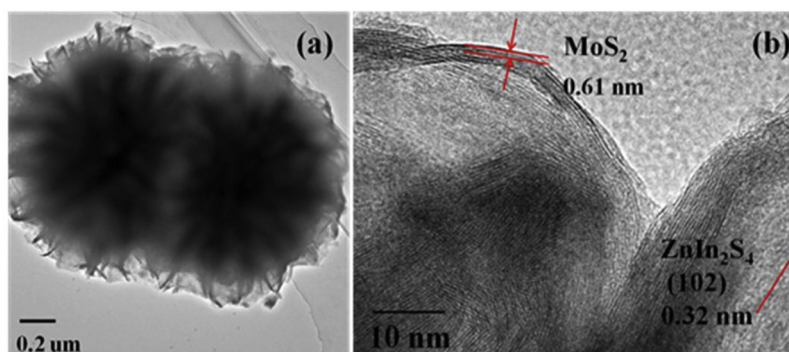

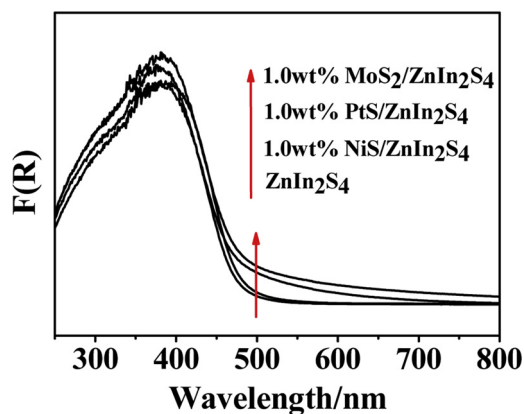**Fig. 3.** 1.0 wt% $MoS_2/ZnIn_2S_4$ nanocomposite (a) TEM image; (b) HRTEM image.

Fig. 4. UV–vis DRS spectra of bare $ZnIn_2S_4$, 1.0 wt% $MoS_2/ZnIn_2S_4$, 1.0 wt% $NiS/ZnIn_2S_4$ and 1.0 wt% $PtS/ZnIn_2S_4$ nanocomposites.

Fig. 5. Time-dependent changes of the amounts of 1,2,3,4-tetra-hydroisoquinoline and the products over irradiated 1.0 wt% $MoS_2/ZnIn_2S_4$ nanocomposite.

Table 1

Photocatalytic dehydrogenation of 1,2,3,4-tetrahydroisoquinoline over 1.0 wt% $MoS_2/ZnIn_2S_4$ nanocomposite under different condition.

Entry	Solvent	Conv. (%)[a]	Yield(%)[b]		Yield of H_2 (%)[c]
			2	3	
1	H_2O	83	81	2	95
2	H_2O	ND	–	–	ND
3	H_2O	ND	–	–	ND
4[d]	H_2O	65	60	5	85
5	CH_3CN	86	80	6	94
6	$CH_3CN:H_2O = 1:1$	90	82	8	96
7	$CH_3CN:H_2O = 2:1$	94	85	9	95
8	$CH_3CN:H_2O = 3:1$	92	86	6	89
9	$DMSO:H_2O = 2:1$	84	80	4	91
10	$EtOH:H_2O = 2:1$	81	75	6	98

Reaction conditions: 1,2,3,4-tetrahydroisoquinoline (0.1 mmol), Catalyst:1.0 wt% $MoS_2/ZnIn_2S_4$ (10 mg), Solvent (2 ml), RT, under N_2 atmosphere, Visible light, Reaction time: 12 h, ND: not detected; [a,b] The products 3,4-dihydroisoquinoline and isoquinoline determined by GC and GC/MS; [c] H_2 Determined by GC.[d] The catalyst is bare $ZnIn_2S_4$.

the dehydrogenation of 1,2,3,4-tetrahydroisoquinoline to generate 3,4-dihydroisoquinoline is really induced by photocatalysis over $ZnIn_2S_4$, while MoS_2 acts as a cocatalyst to promote this reaction (Table 1, entry 4).

Solvent influences only slightly on the performance of this reaction. Although the change of the solvent to CH_3CN leads to a slightly improved conversion (86%) of 1,2,3,4-tetrahydroisoquinoline, the yield to 3,4-dihydroisoquinoline remains at ca. 80% (Table 1, entry 5). The dehydrogenations of 1,2,3,4-tetrahydroisoquinoline in mixed solvents containing CH_3CN, DMF, DMSO, EtOH, respectively, with H_2O were also investigated (Table 1, entries 6–10). Among all the solvents investigated, a mixed solvent containing CH_3CN and H_2O in 2:1 (v/v) ratio gave the best performance by showing a conversion (94%) of 1,2,3,4-tetrahydroisoquinoline in 12 h, with 85% of 3,4-dihydroisoquinoline generated and quantitative hydrogen produced in the meantime (Table 1, entry 7).

Time-dependent conversion of 1,2,3,4-tetrahydroisoquinoline and the formation of the products over 1.0 wt% $MoS_2/ZnIn_2S_4$ in a mixed solvent of CH_3CN: H_2O (2:1) was also investigated (Fig. 5). It was found that the amount of 1,2,3,4-tetrahydroisoquinoline decreased continuously with the irradiation time, with an almost complete conversion (94%) of 1,2,3,4-tetrahydroisoquinoline achieved in 8 h. In the
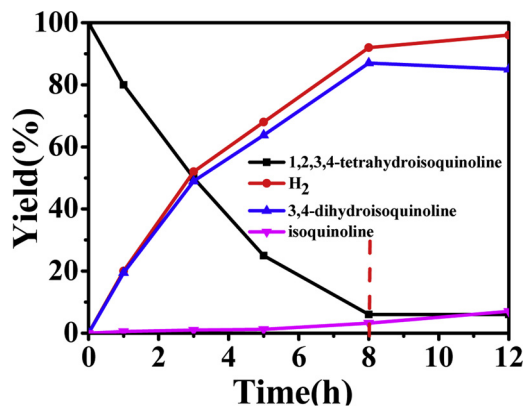
meantime, the yield to 3,4-dihydroisoquinoline increased, with a maximum yield of 87% to 3,4-dihydroisoquinoline achieved at 8 h as well as a yield to isoquinoline at 7%. A extension of the reaction time to 12 h only led to a slightly decreased yield (85%) to 3,4-dihydroisoquinoline, accompanied by a slightly increased yield (9%) to isoquinoline, indicating a very slow transformation of 3,4-dihydroisoquinoline to produce isoquinoline. During the whole reaction process, almost quantitative H_2 was evolved. These observations clearly suggest that the dehydrogenation of 1,2,3,4-tetrahydroisoquinoline proceeds via a two-step process with obviously different reaction rate, i.e, a fast dehydrogenation of two protons in 1,2,3,4-tetrahydroisoquinoline to produce 3,4-dihydroisoquinoline and a very slow step in the transformation of 3,4-dihydroisoquinoline to generate isoquinoline and another molecule of H_2. This result is consistent with that reported previously, which also suggested that the dehydrogenation of 1,2,3,4-tetrahydroisoquinoline to produce isoquinoline proceeds via a two-step process over $[Ru(bpy)_3]Cl_2$ (bpy = 2,2′-bipyridine) [10]. The above observations clearly indicated the feasibility to generate 3,4-dihydroisoquinoline via semi-dehydrogenation of 1,2,3,4-tetrahydroisoquinoline over irradiated $MoS_2/ZnIn_2S_4$ nanocomposite via a careful optimization of the reaction condition

To elucidate the photocatalytic mechanism, several control experiments were carried out. The addition of 0.5 equivalent of 2,2,6,6-tetramethylpiperidine-1-oxyl (TEMPO), a radical scavenger, into the reaction system, led to a significantly decreased activity. Only 40% of 1,2,3,4-tetrahydroisoquinoline was converted to 3,4-dihydroisoquinoline in otherwise similar reaction conditions. This suggested that radical is involved in the photocatalytic dehydrogenation of 1,2,3,4-tetrahydroisoquinoline over $MoS_2/ZnIn_2S_4$, an observation in consistence with previous reports on photocatalytic dehydrogenation of 1,2,3,4-tetrahydroisoquinoline to produce isoquinoline over $[Ru-(bpy)_3]Cl_2$ (bpy = 2,2′-bipyridine) [10] and *h*-BCN [23]. To study the origin of the evolved H_2, D_2O was used to replace H_2O in the reaction. Only H_2 instead of D_2 was detected in the gaseous product, indicating that H_2 generated in the system comes from 1,2,3,4-tetrahydroisoquinoline instead of H_2O.

Based on the above observations and previous studies on dehydrogenation of 1,2,3,4-tetrahydroisoquinoline [10,23], a possible mechanism for photocatalytic semidehydrogenation of 1,2,3,4-tetrahydroisoquinoline to form 3,4-dihydroisoquinoline over $MoS_2/ZnIn_2S_4$ nanocomposite was proposed (Scheme 1). First, 1,2,3,4-tetrahydroisoquinoline is adsorbed on the surface of $ZnIn_2S_4$. When $MoS_2/ZnIn_2S_4$ is irradiated with visible light, electrons and holes are generated over on $ZnIn_2S_4$, in which the photogenerated electrons are transferred to the surface deposited MoS_2 nanoparticles. The surface adsorbed 1,2,3,4-tetrahydroisoquinoline can react with the photogenerated hole in $ZnIn_2S_4$ to produce a radical cation intermediate (A),
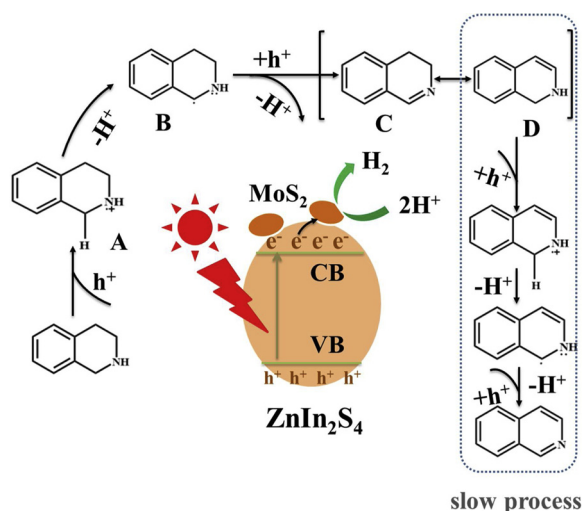
Scheme 1. Proposed mechanism for acceptorless photocatalytic dehydrogenation of 1,2,3,4-tetrahydroisoquinoline under visible light over MoS$_2$/ZnIn$_2$S$_4$ nanocomposite.

Fig. 7. Powder XRD of (a) fresh 1.0 wt% MoS$_2$/ZnIn$_2$S$_4$ and (b) used 1.0 wt% MoS$_2$/ZnIn$_2$S$_4$ composite (after three cycling reactions).

which followed by deprotonation to produce a radical anion intermediate (B). The addition of another hole to B followed by the deprotonation leads to the formation of 3,4-dihydroisoquinoline (C), the semi-dehydrogenated product. In the meantime, the reduction of the protons occurs on MoS$_2$, which acts as the hydrogen evolution cocatalyst. Although tautomerization of 3,4-dihydroisoquinoline (C) to produce energetically equal (D) may allow a second dehydrogenation process to generate the fully deprotonated isoquinoline, this process is not thermodynamically favorable over irradiated ZnIn$_2$S$_4$ due to its less positive valence band potential.

A cycling test showed that there was no obvious loss of photocatalytic activity after three reaction runs (Fig. 6). Besides this, the XRD of the photocatalyst after the reaction did not show much change (Fig. 7). All these suggest that MoS$_2$/ZnIn$_2$S$_4$ nanocomposite is stable during the acceptorless photocatalytic semi-dehydrogenation of 1,2,3,4-tetrahydroisoquinoline to produce 3,4-dihydroisoquinoline.

In addition to MoS$_2$/ZnIn$_2$S$_4$, a series of MS/ZnIn$_2$S$_4$ nanocomposites (MS = PtS and NiS) were also found to show superior performance for the acceptorless photocatalytic semi-dehydrogenation of 1,2,3,4-tetrahydroisoquinoline to form 3,4-dihydroisoquinoline (Table 2). This indicates that coupled with suitable cocatalysts for hydrogen evolution, ZnIn$_2$S$_4$-based nanocomposites show high potential for acceptorless photocatalytic semi-dehydrogenation of 1,2,3,4-tetrahydroisoquinoline to synthesize 3,4-dihydroisoquinoline.
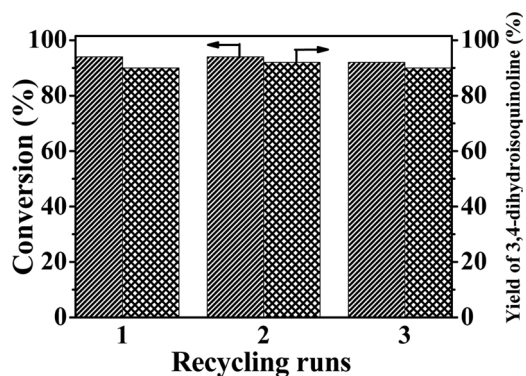
Table 2

Photocatalytic dehydrogenation of 1,2,3,4-tetrahydroisoquinoline over different ZnIn$_2$S$_4$-based nanocomposites.

Entry	Catalyst	Conv.(%)[a]	Yield.(%)[b]		Yield of H$_2$(%)[c]
			2	3	
1	1.0 wt%PtS/ZnIn$_2$S$_4$	76	73	3	80
2	1.0 wt%NiS/ZnIn$_2$S$_4$	83	81	2	85
3	1.0 wt%MoS$_2$/ZnIn$_2$S$_4$	94	85	9	95

Reaction conditions: 1,2,3,4-tetrahydroisoquinoline(0.1 mmol), Catalyst (10 mg), Solvent (2 ml): Solvent (2 ml): CH$_3$CN/H$_2$O (2:1, v/v), RT, under N$_2$ atmosphere, Visible light, Reaction time: 12 h; [a,b] The products 3,4-dihydroisoquinoline and isoquinoline determined by GC and GC/MS; [c] H$_2$ determined by GC.

6. Conclusions

In summary, MoS$_2$ was deposited on the surface of ZnIn$_2$S$_4$ via a photoreduction process and the resultant noble-metal-free MoS$_2$/ZnIn$_2$S$_4$ nanocomposite showed superior performance for acceptorless photocatalytic semi-dehydrogenation of 1,2,3,4-tetrahydroisoquinoline to produce 3,4-dihydroisoquinoline with concomitant generation of hydrogen under visible light. MoS$_2$/ZnIn$_2$S$_4$ nanocomposite is stable during the reaction and can be easily separated for recycling. In addition to MoS$_2$/ZnIn$_2$S$_4$, a series of MS/ZnIn$_2$S$_4$ nanocomposites (MS = PtS and NiS) were also found to show superior performance for this reaction, indicating ZnIn$_2$S$_4$ based nanocomposites are effective photocatalysts for semi-dehydrogenation of 1,2,3,4-tetrahydroisoquinoline to produce 3,4-dihydroisoquinoline. This study not only provides an efficient, green and cost effective method for the synthesis of 3,4-dihydroisoquinoline, but also highlights the great potential of semiconductor-based photocatalysis for light-driven organic syntheses.

Fig. 6. Recycling of 1.0 wt% MoS$_2$/ZnIn$_2$S$_4$ for the dehydrogenation of 1,2,3,4-tetrahydroisoquinoline.

References

[1] W. Liu, S. Liu, R. Jin, H. Guo, J. Zhao, Org. Chem. Front. 2 (2015) 288.
[2] M.M. Heravi, S. Khaghaninejad, N. Nazari, Adv. Heterocycl. Chem. 112 (2014) 183–234.
[3] M. Chrzanowska, M.D. Rozwadowska, Chem. Rev. 104 (2004) 3341–3370.
[4] J.D. Scott, R.M. Williams, Chem. Rev. 102 (2002) 1669–1730.
[5] K. He, W. Zhang, M. Yang, K. Tang, M. Qu, Y. Ding, Y. Li, Org. Lett. 18 (2016) 2840–2843.
[6] R. Kumar, E.H. Gleißner, E.G.V. Tiu, Y. Yamakoshi, Org. Lett. 18 (2016) 184–187.
[7] H. Robert Crabtree, Chem. Rev. 117 (2017) 9228–9246.
[8] K. He, F. Tan, C. Zhou, G. Zhou, X. Yang, Y. Li, Angew. Chem. Int. Ed. 56 (2017) 3080–3084.
[9] Y. Ji, M. Chen, L. Shi, Y. Zhou, Chin. J. Catal. 36 (2015) 33–39.
[10] S. Chen, Q. Wan, A.K. Badu-Tawiah, Angew. Chem. Int. Ed. 55 (2016) 9345–9349.
[11] G. Delaittre, A.S. Goldmann, J.O. Mueller, C. BarnerKowollik, Angew. Chem. Int. Ed. 54 (2015) 11388–11403.
[12] H. Kisch, Angew. Chem. Int. Ed. 52 (2013) 812–847.
[13] X. Lang, X. Chen, J. Zhao, Chem. Soc. Rev. 43 (2014) 473–486.
[14] X. Deng, Z. Li, H. García, Chem.-Eur. J. 23 (2017) 11189–11209.
[15] L. Ye, Z. Li, ChemCatChem 6 (2014) 2540–2543.
[16] X. Lang, X. Ji, H. Chen, C. Chen, W. Ma, J. Zhao, Angew. Chem. Int. Ed. 50 (2011) 3934–3937.
[17] H. Tian, K. Shen, X. Hu, L. Qiao, W. Zheng, J. Alloys. Compd. 691 (2017) 369–377.
[18] M. Kojima, M. Kanai, Angew. Chem. Int. Ed. 55 (2016) 12224–12227.
[19] D. Talwar, A. Gonzalez-de-Castro, H. Li, J. Xiao, Angew. Chem. Int. Ed. 54 (2015) 5223–5227.
[20] S. Chakraborty, W. Brennessel, W. Jones, J. Am. Chem. Soc. 136 (2014) 8564–8567.
[21] J. Hong, Y. Wang, Y. Wang, W. Zhang, R. Xu, ChemSusChem 6 (2013) 2263–2268.
[22] Y. Hong, J. Zhang, F. Huang, J. Zhang, X. Wang, Z. Wu, Z. Lin, J. Yu, J. Mater. Chem. A Mater. Energy Sustain. 3 (2015) 13913–13919.
[23] M. Zheng, J. Shi, T. Yuan, X. Wang, Angew. Chem. Int. Ed. 57 (2018) 5487–5491.
[24] L. Ye, J. Fu, Z. Xu, R. Yuan, Z. Li, A.C.S. Appl, Mater. Inter. 6 (2014) 3483–3490.
[25] Y. Chen, S. Hu, W. Liu, X. Chen, L. Wu, X. Wang, P. Liu, Z. Li, Dalton Trans. 40 (2011) 2607–2613.
[26] S. Shen, L. Zhao, Z. Zhou, J. Guo, J. Phys. Chem. C. 112 (2008) 16148–16155.
[27] Y. Li, J. Wang, S. Peng, G. Lu, S. Li, Int. J. Hydrogen Energy 35 (2010) 7116–7126.
[28] B. Wang, Z. Deng, X. Fu, Z. Li, J. Mater. Chem. A Mater. Energy Sustain. 6 (2018) 19735.
[29] Y. Yuan, J. Tu, Z. Ye, D. Chen, B. Hu, Y. Huang, T. Chen, D. Cao, Z. Yu, Z. Zou, Appl. Catal. B: Environ. 188 (2016) 13–22.
[30] Q. Xiang, J. Yu, M. Jaroniec, J. Am. Chem. Soc. 134 (2012) 6575–6578.
[31] L. Wei, Y. Chen, Y. Lin, H. Wu, R. Yuan, Z. Li, Appl. Catal. B: Environ. 144 (2014) 521–527.
[32] A. Wu, C. Tian, H. Yan, H. Jiao, Q. Yan, G. Yang, H. Fu, Nanoscale 8 (2016) 11052–11059.
[33] H. Tian, H. Liu, W. Zheng, Appl. Catal. B 225 (2018) 468–476.
[34] M. Liu, X. Xue, S. Yu, X. Wang, X. Hu, H. Tian, H. Chen, W. Zheng, Sci. Rep. 7 (2017) 3637.
[35] D. Genuit, P. Afanasiev, M. Vrinat, J. Catal. 235 (2005) 302–317.
[36] L. Xu, X. Deng, Z. Li, Appl. Catal. B: Environ. 234 (2018) 50–55.
[37] L. Wei, Y. Chen, J. Zhao, Z. Li, Beilstein J. Nanotech. 4 (2013) 949–955.
[38] Y. Ding, Y. Gao, Z. Li, Appl. Surf. Sci. 462 (2018) 255–262.